

DOI: 10.11830/ISSN.1000-5013.202011026



# 重心插值配点法求解 Cahn-Hilliard 方程

邓杨芳, 黄蓉, 翁智峰

(华侨大学 数学科学学院, 福建 泉州 362021)

**摘要:** 对 Cahn-Hilliard 方程中的时、空方向均采用重心插值配点格式(重心 Lagrange 插值配点格式和重心有理插值配点格式)进行离散,非线性项采用一般迭代法,导出离散的线性代数方程组,并给出重心 Lagrange 插值的逼近误差估计.数值算例表明:两种重心插值配点格式均具有高精度,且满足能量递减规律.

**关键词:** Cahn-Hilliard 方程; 重心插值配点格式; 迭代格式; 能量递减

中图分类号: O 241.82

文献标志码: A

文章编号: 1000-5013(2022)01-0135-10

## Barycentric Interpolation Collocation Method for Cahn-Hilliard Equation

DENG Yangfang, HUANG Rong, WENG Zhifeng

(School of Mathematical Sciences, Huaqiao University, Quanzhou 362021, China)

**Abstract:** Barycentric interpolation collocation schemes (barycentric Lagrange interpolation collocation scheme and barycentric rational interpolation collocation scheme) are used to discretize both in time and in space for Cahn-Hilliard equation. The general iteration method is used for the nonlinear term, which derives the discrete linear algebraic equations. Moreover, the error estimation of barycentric Lagrange interpolation method is given. Numerical examples show the high accuracy and the law of energy decline satisfied to the two collocation schemes.

**Keywords:** Cahn-Hilliard equation; barycentric interpolation collocation scheme; iterative scheme; energy decline

1958 年, Cahn 等<sup>[1]</sup>在研究热力学两相物质(如合金、聚合物等)之间的相互扩散现象时,提出 Cahn-Hilliard 方程. Cahn-Hilliard 方程是一类重要的四阶非线性扩散方程,用来描述固体表面上微滴的扩散、河床的迁移、生物种群的竞争与排斥等扩散现象,也广泛应用于工程流体力学<sup>[2-3]</sup>、材料科学<sup>[4]</sup>、图像分析<sup>[5-6]</sup>和生命科学<sup>[7-8]</sup>等领域.国内外学者对 Cahn-Hilliard 方程提出了许多数值解法,如有限差分<sup>[9-11]</sup>、有限元<sup>[12-13]</sup>、有限体积<sup>[14]</sup>、谱方法<sup>[15-16]</sup>等. Zhang 等<sup>[17]</sup>构造一个无条件能量稳定的有限差分格式,并基于该格式提出自适应时间步长策略. Cheng 等<sup>[18]</sup>采用快速稳定的显式算子分裂方法求解 Cahn-Hilliard 方程. Li 等<sup>[19]</sup>考虑求解二维 Cahn-Hilliard 方程的半隐稳定化傅里叶谱方法,并对几种经典的稳定化技术进行比较研究,确定相应的稳定区域. Cheng 等<sup>[20]</sup>提出一个能量稳定的四阶差分格式求解带周期边界条件的 Cahn-Hilliard 方程,并证明该格式解的唯一性和能量稳定性. Wang 等<sup>[21]</sup>提出一个能量稳定的线性扩散 Crank-Nicolson 格式求解 Cahn-Hilliard 方程. Zhang 等<sup>[22]</sup>构造一类无条件能量

收稿日期: 2020-11-26

通信作者: 翁智峰(1985-),男,副教授,博士,主要从事偏微分方程数值解的研究. E-mail: zfwmath@163.com.

基金项目: 国家自然科学基金资助项目(11701197); 中央高校基本科研业务费专项资金资助项目(ZQN-702)

稳定的线性二阶预估-校正时间步进格式求解 Cahn-Hilliard 方程.

上述方法都是基于网格剖分求解微分方程问题. 李淑萍等<sup>[23]</sup>利用重心插值配点法求解微分方程初边值问题, 重心插值配点法包括重心 Lagrange 插值和重心有理插值. 对于等距插值节点, 高阶 Lagrange 插值公式构造的近似函数值容易出现 Runge 现象, 具有极大的数值不稳定性. 为了避免这一现象的出现, Berrut 等<sup>[24]</sup>分别将 Lagrange 插值公式改为重心 Lagrange 插值和重心有理插值<sup>[25]</sup>, 克服数值格式的振荡现象. 重心插值配点法作为一种新型的无网格计算方法, 具有计算格式简单、精度高、程序实施方便、节点适应性好等特点, 使用 Chebyshev 节点有效克服了 Runge 现象. 重心插值配点法被推广到求解各类积分和微分方程, 如高维 Fredholm 积分方程<sup>[26]</sup>、非线性抛物方程<sup>[27]</sup>、粘弹性波方程<sup>[28]</sup>、Allen-Cahn 方程<sup>[29-30]</sup>、Black-Scholes 方程<sup>[31]</sup>等. 本文将重心插值配点法推广到求解 Cahn-Hilliard 方程.

## 1 Cahn-Hilliard 方程的重心插值配点法

### 1.1 Cahn-Hilliard 方程

Cahn-Hilliard 方程是相场模型方程之一, 用来模拟二元合金中的相分离现象, 即

$$\varphi_t(x, t) = \Delta(F'(\varphi(x, t)) - \varepsilon^2 \Delta\varphi(x, t)), \quad x \in [a, b], \quad t \in [0, T]. \quad (1)$$

边界条件为

$$\varphi(a, t) = \alpha_1(t), \quad \varphi(b, t) = \alpha_2(t), \quad \varphi'(a, t) = \beta_1(t), \quad \varphi'(b, t) = \beta_2(t). \quad t \in [0, T], \quad (2)$$

初始条件为

$$\varphi(x, 0) = \psi(x), \quad x \in [a, b]. \quad (3)$$

式(1)~(3)中:  $\varphi$  为两种物质之一的密度,  $F(\varphi) = \frac{1}{4}(\varphi^2 - 1)^2$  为双势阱函数;  $\Delta$  是 Laplace 算子;  $\varepsilon$  是一个与界面宽度相关的参数,  $\varepsilon > 0$ .

Cahn-Hilliard 方程也可看作是  $H^{-1}$  内积下的一个梯度流, 它的自由能泛函为

$$E(\varphi) = \int_a^b (F(\varphi) + \frac{\varepsilon^2}{2} |\nabla\varphi|^2) dx. \quad (4)$$

式(4)中:  $\nabla$  是梯度算子.

令  $\mu = F'(\varphi) - \varepsilon^2 \Delta\varphi$ , 方程(1)与  $\mu$  作内积可得

$$E'(t) = (\varphi_t, \mu) = (\Delta\mu, \mu) = - \int_a^b |\nabla\mu|^2 dx \leq 0. \quad (5)$$

因此, Cahn-Hilliard 方程满足能量递减规律, 在采用数值方法求解 Cahn-Hilliard 方程时, 不仅要保证数值精度, 而且要保证能量的稳定性.

### 1.2 重心型插值

1.2.1 重心 Lagrange 插值 设有插值节点  $t_j$  和一组对应的实数  $f_j (j=0, 1, \dots, m)$ , 采用多项式插值, 则在次数不超过  $m$  的多项式空间可以找到唯一的插值多项式  $p(t)$ , 满足  $p(t_j) = f_j, j=0, 1, \dots, m$ , Lagrange 插值公式为

$$p(t) = \sum_{j=0}^m \gamma_j(t) f_j. \quad (6)$$

式(6)中:  $\gamma_j(t) = \prod_{i=0, i \neq j}^m (t - t_i) / \prod_{i=0, i \neq j}^m (t_j - t_i) (j=0, 1, \dots, m)$  为 Lagrange 插值基函数, 性质为

$$\gamma_j(t_i) = \delta_{j,i} = \begin{cases} 1, & j=i, \quad i, j=0, 1, \dots, m, \\ 0, & j \neq i, \quad i, j=0, 1, \dots, m, \end{cases} \quad (7)$$

$$\sum_{j=0}^m \gamma_j(t) = 1. \quad (8)$$

令  $l(t) = (t - t_0)(t - t_1) \cdots (t - t_m)$ , 定义重心权  $w_j = \frac{1}{\prod_{i=0, i \neq j}^m (t_j - t_i)} (j=0, 1, \dots, m)$ , 则插值基函

数可以表示为

$$\gamma_j(t) = l(t) \frac{\omega_j}{t - t_j}, \quad j = 0, 1, \dots, m. \quad (9)$$

将式(9)代入式(6), 有

$$p(t) = l(t) \sum_{j=0}^m \frac{\omega_j}{t - t_j} f_j. \quad (10)$$

由式(8)~(10), 可得重心 Lagrange 插值公式, 即

$$p(t) = \sum_{j=0}^m \frac{\omega_j}{t - t_j} f_j / \sum_{j=0}^m \frac{\omega_j}{t - t_j}. \quad (11)$$

重心 Lagrange 插值对于等距节点是病态的, 通过选用服从密度比为  $(1-t^2)^{-\frac{1}{2}}$  的节点族, 可使其具有非常好的数值稳定性. 满足这样条件的最简单的节点分布是 Chebyshev 点族, 因此, 采用第二类 Chebyshev 点族:  $t_j = \cos\left(\frac{j}{m}\pi\right)$  ( $j=0, 1, \dots, m$ ), 以保证重心 Lagrange 插值的数值稳定性.

1.2.2 重心有理插值 设有插值节点  $t_j$  ( $j=0, 1, \dots, m$ ) 和一组对应的实数  $f_j$ , 选择一个整数  $d$  且满足  $0 \leq d \leq m$ , 令  $p_j(t)$  为插值  $d+1$  个点  $(t_j, f_j), (t_{j+1}, f_{j+1}), \dots, (t_{j+d}, f_{j+d})$  ( $j=0, 1, \dots, m-d$ ) 的次数最多为  $d$  的多项式, 则

$$r(t) = \sum_{j=0}^{m-d} \lambda_j(t) p_j(t) / \sum_{j=0}^{m-d} \lambda_j(t). \quad (12)$$

式(12)中:  $\lambda_j(t) = (-1)^j / ((t-t_j) \cdots (t-t_{j+d}))$ .

将  $p_j(t)$  写成 Lagrange 插值形式, 整理得

$$\sum_{j=0}^{m-d} \lambda_j(t) p_j(t) = \sum_{k=0}^m \frac{\omega_k}{t - t_k} f_k. \quad (13)$$

式(13)中:  $\omega_k = \sum_{j \in J_k} (-1)^j \prod_{i=j, i \neq k}^{j+d} \frac{1}{(t_k - t_i)}$ , 指标集  $J_k = \{j \in \{0, 1, \dots, m\} : k-d \leq j \leq k\}$ .

由于  $1 = \sum_{k=j}^{j+d} \prod_{i=j, i \neq k}^{j+d} \frac{t - t_i}{t_k - t_i}$ , 故有

$$\sum_{j=0}^{m-d} \lambda_j(t) = \sum_{j=0}^{m-d} \lambda_j(t) \cdot 1 = \sum_{k=0}^m \frac{\omega_k}{t - t_k}. \quad (14)$$

将式(13), (14)代入式(12), 得到高阶重心有理插值公式, 即

$$r(t) = \left( \sum_{j=0}^m \frac{\omega_j}{t - t_j} f_j / \sum_{j=0}^m \frac{\omega_j}{t - t_j} \right) =: \sum_{j=0}^m \gamma_j(t) f_j. \quad (15)$$

重心有理插值基于混合函数的思想, 可以有效克服等距插值的不稳定问题.

1.2.3 重心插值的微分矩阵 由式(15), 函数  $r(t)$  在节点  $t_0, t_1, \dots, t_m$  处的  $v$  阶导数为

$$r^{(v)}(t_i) = \frac{d^v r(t_i)}{dt^v} = \sum_{j=0}^m \gamma_j^{(v)}(t_i) f_j = \sum_{j=0}^m D_{i,j}^{(v)} f_j, \quad v = 1, 2, 3, 4. \quad (16)$$

由文献[32], 一阶和二阶微分矩阵的计算公式为

$$\left. \begin{aligned} D_{i,j}^{(1)} &= \gamma_j'(t_i) = \frac{\omega_j / \omega_i}{t_i - t_j}, \quad j \neq i, \\ D_{i,i}^{(1)} &= - \sum_{j=0, j \neq i}^m D_{i,j}^{(1)}, \\ D_{i,j}^{(2)} &= \gamma_j''(t_i) = -2 \frac{\omega_j / \omega_i}{t_i - t_j} \left( \sum_{k \neq i} \frac{\omega_k / \omega_i}{t_i - t_k} + \frac{1}{t_i - t_j} \right), \quad j \neq i, \\ D_{i,i}^{(2)} &= - \sum_{j=0, j \neq i}^m D_{i,j}^{(2)}. \end{aligned} \right\} \quad (17)$$

利用数学归纳法, 可以得到  $v$  阶微分矩阵的递推公式

$$\left. \begin{aligned} D_{i,j}^{(v)} &= v(D_{i,i}^{(v-1)} D_{i,j}^{(1)} - \frac{D_{i,j}^{(v-1)}}{t_i - t_j}), \quad j \neq i, \\ D_{i,i}^{(v)} &= - \sum_{j=0, j \neq i}^m D_{i,j}^{(v)}. \end{aligned} \right\} \quad (18)$$

### 1.3 一般迭代格式下的 Cahn-Hilliard 方程

Cahn-Hilliard 方程的非线性项可以表示为  $\frac{\partial^2(\varphi^3 - \varphi)}{\partial x^2} = (6\varphi\varphi_x)\varphi_x + (3\varphi^2 - 1)\varphi_{xx}$ . 因此, Cahn-Hilliard 方程的一般迭代格式为

$$\varphi_t^{(k+1)} + \varepsilon^2 \varphi_{xxxx}^{(k+1)} - (3(\varphi^{(k)})^2 - 1)\varphi_{xx}^{(k+1)} - (6\varphi^{(k)}\varphi_x^{(k)})\varphi_x^{(k+1)} = 0, \quad k=0, 1, 2, \dots, N-1. \quad (19)$$

式(19)中:  $k$  为迭代次数.

### 1.4 Cahn-Hilliard 方程的重心插值配点格式

引入记号  $s(x, t) = (3(\varphi^{(k)})^2 - 1)$ ,  $g(x, t) = (6\varphi^{(k)}\varphi_x^{(k)})$ ,  $\varphi(x, t) = \varphi^{(k+1)}$ , 则式(19)可简记为

$$\varphi_t + \varepsilon^2 \varphi_{xxxx} - s(x, t)\varphi_{xx} - g(x, t)\varphi_x = 0. \quad (20)$$

首先, 对空间域  $[a, b]$  和时间域  $[0, T]$  进行网格剖分:  $a = x_0 < x_1 < \dots < x_M = b$ ,  $0 = t_0 < t_1 < \dots < t_N = T$ . 记  $\varphi(x_i, t) = \varphi_i(t)$ , 得  $\varphi(x, t)$  在节点  $x_0, x_1, \dots, x_M$  的重心插值函数为

$$\varphi(x, t) = \sum_{l=0}^M \gamma_l(x) \varphi_l(t). \quad (21)$$

将式(21)代入式(20), 使其在点  $x_0, x_1, \dots, x_M$  上成立, 有

$$\sum_{l=0}^M \gamma_l(x_i) \dot{\varphi}_l(t) + \varepsilon^2 \sum_{l=0}^M \gamma_l'''(x_i) \varphi_l(t) - s(x_i, t) \sum_{l=0}^M \gamma_l''(x_i) \varphi_l(t) - g(x_i, t) \sum_{l=0}^M \gamma_l'(x_i) \varphi_l(t) = 0, \quad i = 0, 1, \dots, M. \quad (22)$$

式(22)中:  $\dot{\varphi}_l(t) = \frac{\partial \varphi_l(t)}{\partial t}$ ;  $\gamma_l'''(x_i) = C_{i,l}^{(4)}$ ;  $\gamma_l''(x_i) = C_{i,l}^{(2)}$ ;  $\gamma_l'(x_i) = C_{i,l}^{(1)}$ ;  $C_{i,l}^{(v)}$  ( $v=1, 2, 3, 4$ ) 为节点  $x_0, x_1, \dots, x_M$  上重心插值  $v$  阶微分矩阵的元素.

记  $s(x_i, t) = s_i(t)$ ,  $g(x_i, t) = g_i(t)$ ,  $i = 0, 1, \dots, M$ , 可得方程(22)的矩阵表示形式, 即

$$\begin{bmatrix} \dot{\varphi}_0(t) \\ \vdots \\ \dot{\varphi}_M(t) \end{bmatrix} + \varepsilon^2 \begin{bmatrix} C_{0,0}^{(4)} & \cdots & C_{0,M}^{(4)} \\ \vdots & & \vdots \\ C_{M,0}^{(4)} & \cdots & C_{M,M}^{(4)} \end{bmatrix} \begin{bmatrix} \varphi_0(t) \\ \vdots \\ \varphi_M(t) \end{bmatrix} - \begin{bmatrix} s_0(t) & & \\ & \ddots & \\ & & s_M(t) \end{bmatrix} \begin{bmatrix} C_{0,0}^{(2)} & \cdots & C_{0,M}^{(2)} \\ \vdots & & \vdots \\ C_{M,0}^{(2)} & \cdots & C_{M,M}^{(2)} \end{bmatrix} \begin{bmatrix} \varphi_0(t) \\ \vdots \\ \varphi_M(t) \end{bmatrix} - \begin{bmatrix} g_0(t) & & \\ & \ddots & \\ & & g_M(t) \end{bmatrix} \begin{bmatrix} C_{0,0}^{(1)} & \cdots & C_{0,M}^{(1)} \\ \vdots & & \vdots \\ C_{M,0}^{(1)} & \cdots & C_{M,M}^{(1)} \end{bmatrix} \begin{bmatrix} \varphi_0(t) \\ \vdots \\ \varphi_M(t) \end{bmatrix} = 0. \quad (23)$$

记  $\varphi_i(t_j) = \varphi(x_i, t_j) := \varphi_{i,j}$ , 得到  $\varphi_i(t)$  在点  $t_0, t_1, \dots, t_N$  上的重心插值函数, 即

$$\varphi_i(t) = \sum_{q=0}^N \gamma_q(t) \varphi_{i,q}, \quad i = 0, 1, \dots, M. \quad (24)$$

将式(24)代入式(23), 使其在点  $t_0, t_1, \dots, t_N$  上成立, 有

$$\begin{bmatrix} \sum_{q=0}^N \gamma_q(t_j) \varphi_{0,q} \\ \vdots \\ \sum_{q=0}^N \gamma_q(t_j) \varphi_{M,q} \end{bmatrix} + \varepsilon^2 \begin{bmatrix} C_{0,0}^{(4)} & \cdots & C_{0,M}^{(4)} \\ \vdots & & \vdots \\ C_{M,0}^{(4)} & \cdots & C_{M,M}^{(4)} \end{bmatrix} \begin{bmatrix} \sum_{q=0}^N \gamma_q(t_j) \varphi_{0,q} \\ \vdots \\ \sum_{q=0}^N \gamma_q(t_j) \varphi_{M,q} \end{bmatrix} - \begin{bmatrix} s_0(t_j) & & \\ & \ddots & \\ & & s_M(t_j) \end{bmatrix} \begin{bmatrix} C_{0,0}^{(2)} & \cdots & C_{0,M}^{(2)} \\ \vdots & & \vdots \\ C_{M,0}^{(2)} & \cdots & C_{M,M}^{(2)} \end{bmatrix} \begin{bmatrix} \sum_{q=0}^N \gamma_q(t_j) \varphi_{0,q} \\ \vdots \\ \sum_{q=0}^N \gamma_q(t_j) \varphi_{M,q} \end{bmatrix} - \begin{bmatrix} g_0(t_j) & & \\ & \ddots & \\ & & g_M(t_j) \end{bmatrix} \begin{bmatrix} C_{0,0}^{(1)} & \cdots & C_{0,M}^{(1)} \\ \vdots & & \vdots \\ C_{M,0}^{(1)} & \cdots & C_{M,M}^{(1)} \end{bmatrix} \begin{bmatrix} \sum_{q=0}^N \gamma_q(t_j) \varphi_{0,q} \\ \vdots \\ \sum_{q=0}^N \gamma_q(t_j) \varphi_{M,q} \end{bmatrix} = 0.$$

$$\begin{bmatrix} g_0(t_j) & & \\ & \ddots & \\ & & g_M(t_j) \end{bmatrix} \begin{bmatrix} C_{0,0}^{(1)} & \cdots & C_{0,M}^{(1)} \\ \vdots & & \vdots \\ C_{M,0}^{(1)} & \cdots & C_{M,M}^{(1)} \end{bmatrix} \begin{bmatrix} \sum_{q=0}^N \gamma_q(t_j) \varphi_{0,q} \\ \vdots \\ \sum_{q=0}^N \gamma_q(t_j) \varphi_{M,q} \end{bmatrix} = 0, \quad j = 0, 1, \dots, N. \quad (25)$$

式(25)中:  $\dot{\gamma}_q(t_j) = \frac{d\gamma_q(t_j)}{dt} = D_{j,q}^{(1)}$ ,  $D_{j,q}^{(1)}$  为节点  $t_0, t_1, \dots, t_N$  上重心插值 1 阶微分矩阵的元素. 令

$$\boldsymbol{\varphi}_i = [\varphi_{i,0}, \varphi_{i,1}, \dots, \varphi_{i,N}]^T,$$

$$\mathbf{s}_i = \text{diag}(s_{i,0}, s_{i,1}, \dots, s_{i,N}) = \text{diag}(s_i(t_0), s_i(t_1), \dots, s_i(t_N)),$$

$$\mathbf{g}_i = \text{diag}(g_{i,0}, g_{i,1}, \dots, g_{i,N}) = \text{diag}(g_i(t_0), g_i(t_1), \dots, g_i(t_N)), \quad i = 0, 1, \dots, M.$$

方程(25)可以简记为矩阵形式, 即

$$\begin{aligned} (\mathbf{I}_M \otimes \mathbf{D}^{(1)}) \begin{bmatrix} \boldsymbol{\varphi}_0 \\ \vdots \\ \boldsymbol{\varphi}_M \end{bmatrix} + (\varepsilon^2 (\mathbf{C}^{(4)} \otimes \mathbf{I}_N) - \begin{bmatrix} \mathbf{s}_0 & & \\ & \ddots & \\ & & \mathbf{s}_M \end{bmatrix} (\mathbf{C}^{(2)} \otimes \mathbf{I}_N) - \\ \begin{bmatrix} \mathbf{g}_0 & & \\ & \ddots & \\ & & \mathbf{g}_M \end{bmatrix} (\mathbf{C}^{(1)} \otimes \mathbf{I}_N)) \begin{bmatrix} \boldsymbol{\varphi}_0 \\ \vdots \\ \boldsymbol{\varphi}_M \end{bmatrix} = 0. \end{aligned} \quad (26)$$

式(26)中: 符号  $\otimes$  代表矩阵的 Kronecker 积;  $\mathbf{I}_M, \mathbf{I}_N$  分别为  $M+1, N+1$  阶单位矩阵;  $\mathbf{C}^{(v)}, \mathbf{D}^{(v)}$  ( $v=1, 2, 3, 4$ ) 分别表示节点  $x_0, x_1, \dots, x_M$  和  $t_0, t_1, \dots, t_N$  上的重心插值  $v$  阶微分矩阵. 设

$$\boldsymbol{\varphi} = [\boldsymbol{\varphi}_0^T, \boldsymbol{\varphi}_1^T, \dots, \boldsymbol{\varphi}_M^T], \quad \mathbf{s} = \begin{bmatrix} \mathbf{s}_0 & & \\ & \ddots & \\ & & \mathbf{s}_M \end{bmatrix}, \quad \mathbf{g} = \begin{bmatrix} \mathbf{g}_0 & & \\ & \ddots & \\ & & \mathbf{g}_M \end{bmatrix},$$

则式(26)可以表示为

$$[(\mathbf{I}_M \otimes \mathbf{D}^{(1)}) + \varepsilon^2 (\mathbf{C}^{(4)} \otimes \mathbf{I}_N) - \mathbf{s} (\mathbf{C}^{(2)} \otimes \mathbf{I}_N) - \mathbf{g} (\mathbf{C}^{(1)} \otimes \mathbf{I}_N)] \boldsymbol{\varphi} = 0. \quad (27)$$

类似地, 采用重心插值格式逼近  $s(x, t)$  和  $g(x, t)$ , 得到 Cahn-Hilliard 方程在重心插值配点法下的迭代计算格式, 即

$$\begin{aligned} [(\mathbf{I}_M \otimes \mathbf{D}^{(1)}) + \varepsilon^2 (\mathbf{C}^{(4)} \otimes \mathbf{I}_N) - \text{diag}(3(\boldsymbol{\varphi}^{(k)})^2 - 1) (\mathbf{C}^{(2)} \otimes \mathbf{I}_N) - \\ \text{diag}(6\boldsymbol{\varphi}^{(k)} ((\mathbf{C}^{(1)} \otimes \mathbf{I}_N) \boldsymbol{\varphi}^{(k)})) (\mathbf{C}^{(1)} \otimes \mathbf{I}_N)] \boldsymbol{\varphi}^{(k+1)} = 0. \end{aligned} \quad (28)$$

### 1.5 插值误差估计

由插值逼近误差理论估计最后的误差范围, 有助于检验算法在计算过程中的整体误差结果. 由文献 [33] 的定理 3.1, 得到定理 1.

**定理 1** 如果  $\varphi(x, t) \in C^{n+1}(\Omega)$ ,  $\Omega = [a, b] \times (0, T] \in \mathbf{R}^2$  是一个带 Lipschitz 连续边界的非空开集,  $\varphi^h(x, t)$  为  $\varphi(x, t)$  的重心 Lagrange 插值函数, 则有如下误差估计成立, 即

$$\max |\varphi(x, t) - \varphi^h(x, t)| \leq \| \varphi^{(n+1)} \|_\infty \left\{ c_x \left( \frac{e(b-a)}{2M} \right)^M + c_t \left( \frac{eT}{2N} \right)^N \right\}, \quad (29)$$

$$\max \left| \frac{\partial^4 \varphi(x, t)}{\partial x^4} - \frac{\partial^4 \varphi^h(x, t)}{\partial x^4} \right| \leq c_x^* \| \varphi^{(n+1)} \|_\infty \left( \frac{e(b-a)}{2(M-4)} \right)^{M-4}, \quad (30)$$

$$\max \left| \frac{\partial \varphi(x, t)}{\partial t} - \frac{\partial \varphi^h(x, t)}{\partial t} \right| \leq c_t^* \| \varphi^{(n+1)} \|_\infty \left( \frac{eT}{2(N-1)} \right)^{N-1}. \quad (31)$$

式(29)~(31)中:  $e$  是自然对数;  $c_x, c_x^*, c_t^*$  均表示大于 0 的任意常数.

证明: 设  $x_i (i=0, 1, \dots, M)$  为区间  $[-1, 1]$  上的 Chebyshev 节点,  $x_0 = 1, x_M = -1, \varphi(x) \in C^{n+1}(-1, 1)$ , 由文献 [33], 有

$$\left| \prod_{i=0}^M (x - x_i) \right| \leq M2^{1-M}. \quad (32)$$

由拉格朗日插值余项定理, 有

$$\varphi^{(v)}(x) - (\varphi^h(x))^{(v)} = \frac{\varphi^{(m+1)}(\xi_i)}{(M+1-v)!} \prod_{i=0}^{M-v} (x-x_i). \quad (33)$$

式(33)中: $v$ 表示求导的次数, $v=1,2,3,4$ .

当 $M \gg 1$ 时,由 Stirling 公式知

$$\Gamma(M+1) = M! \cong \sqrt{2\pi} M^{M+1/2} e^{-M}. \quad (34)$$

结合式(32)~(34),有

$$\max_{x \in (-1,1)} |\varphi - \varphi^h| \leq c_0 \|\varphi^{(m+1)}\|_{\infty} \left(\frac{e}{2M}\right)^M, \quad (35)$$

$$\max_{x \in (-1,1)} \left| \frac{d^v \varphi}{dx^v} - \frac{d^v \varphi^h}{dx^v} \right| \leq c_1 \|\varphi^{(m+1)}\|_{\infty} \left(\frac{e}{2(M-v)}\right)^{M-v}. \quad (36)$$

式(36)中:当 $n$ 较大时, $c_0, c_1$ 是与 $M$ 无关的常数.

对 $x \in [a, b]$ ,引入坐标变换: $x^* = \frac{2(x-a)}{b-a} - 1 \in [-1, 1]$ ,由式(35),(36),有

$$\max_{x \in (a,b)} |\varphi - \varphi^h| \leq c_0^* \|\varphi^{(m+1)}\|_{\infty} \left(\frac{e(b-a)}{2M}\right)^M, \quad (37)$$

$$\max_{x \in (a,b)} \left| \frac{d^v \varphi}{dx^v} - \frac{d^v \varphi^h}{dx^v} \right| \leq c_1^* \|\varphi^{(m+1)}\|_{\infty} \left(\frac{e(b-a)}{2(M-v)}\right)^{M-v}. \quad (38)$$

对于二元函数 $\varphi(x, t)$ ,有

$$\begin{aligned} |\varphi(x, t) - \varphi^h(x_m, t) + \varphi^h(x_m, t) - \varphi^h(x_m, t_n)| &\leq |\varphi(x, t) - \varphi^h(x_m, t)| + |\varphi^h(x_m, t) - \varphi^h(x_m, t_n)| \\ &\leq \|\varphi^{(n+1)}\|_{\infty} \left\{ c_x \left(\frac{e(b-a)}{2M}\right)^M + c_t \left(\frac{eT}{2N}\right)^N \right\}. \end{aligned} \quad (39)$$

即有式(29)成立.取 $v=4$ ,由式(38)即可得到式(30),同理可得式(31).

从逼近误差结果可知,该算法是指数收敛的,且微分算子的阶数决定了代数方程的收敛阶.

## 2 数值算例

给出两个数值算例来验证重心插值配点格式的高精度和有效性.记 $u^h, u$ 分别为数值解和真解向量,定义相对误差和绝对误差分别为

$$E_a = \|u^h - u\|_{\infty}, \quad E_r = \frac{\|u^h - u\|_{\infty}}{\|u\|_{\infty}}. \quad (40)$$

式(40)中: $\|\cdot\|_{\infty}$ 表示无穷范数.

### 2.1 算例 1

为对比两种重心插值配点格式的精度,选取三角函数精确解的方程作为测试实例.考虑 Cahn-Hilliard 方程,即

$$\left. \begin{aligned} \varphi_t + \varepsilon^2 \frac{\partial^4 \varphi}{\partial x^4} - \frac{\partial^2 (\varphi^3 - \varphi)}{\partial x^2} &= f(x), \quad x \in [-1, 1], \quad t \in [0, 1], \\ \varphi(x, 0) &= \sin^2(\pi x), \quad x \in [-1, 1], \\ \varphi(-1, t) = \varphi'(1, t) &= 0, \quad t \in [0, 1], \\ \varphi(1, t) = \varphi'(-1, t) &= 0, \quad t \in [0, 1]. \end{aligned} \right\} \quad (41)$$

式(41)中: $\varphi = \sin^2(\pi x) \cos(t)$ ;  $f(x) = -\sin^2(\pi x) \sin(t) - 2\pi^2 \cos(t) (4\pi^2 \varepsilon^2 + 3\sin^4(\pi x) \cos^2(t) - 1) (\cos^2(\pi x) - \sin^2(\pi x)) - 24\pi^2 \sin^4(\pi x) \cos^2(\pi x) \cos^3(t)$ .

当 $\varepsilon=0.3$ 时,求解问题(41),重心 Lagrange 插值配点格式和重心有理插值配点格式的误差比较,如表 1 所示.由表 1 可知:节点数量在一定范围内增加时,两种重心插值配点格式的计算误差与节点数量之间呈指数下降,取较少节点数时,如 $M=20, 25, N=10, 10$ ,重心 Lagrange 插值配点格式的精度高于重心有理插值配点格式的精度;随着计算节点的进一步增加,两种重心插值配点格式的绝对误差 $E_a$ 和相对误差 $E_r$ 都出现微小振荡,重心有理插值配点的表现更平稳,但仍都维持在 $10^{-11}$ 和 $10^{-10}$ 量级;两种重心插值配点格式都具有很高的计算精度和较好的数值稳定性;综合比较可知,重心 Lagrange 插值配点格式的精度更高,重心有理插值配点格式的数值稳定性更好.

表 1 两种重心插值配点格式的误差比较

Tab. 1 Error comparison of two barycentric interpolation collocation formats

M	N	重心 Lagrange 插值配点格式		重心有理插值配点格式	
		$E_a$	$E_r$	$E_a$	$E_r$
20	10	$2.5216 \times 10^{-8}$	$2.5751 \times 10^{-8}$	$8.4303 \times 10^{-7}$	$8.6089 \times 10^{-7}$
25	10	$2.1156 \times 10^{-11}$	$2.1426 \times 10^{-11}$	$1.1057 \times 10^{-8}$	$1.1198 \times 10^{-8}$
30	15	$2.0832 \times 10^{-10}$	$2.0832 \times 10^{-10}$	$1.7060 \times 10^{-11}$	$1.7060 \times 10^{-11}$
30	20	$4.6657 \times 10^{-11}$	$4.6657 \times 10^{-11}$	$3.8379 \times 10^{-11}$	$3.8379 \times 10^{-11}$
35	25	$9.7093 \times 10^{-11}$	$9.7750 \times 10^{-11}$	$1.2098 \times 10^{-10}$	$1.2180 \times 10^{-10}$

取  $M=25, N=15$ , 重心 Lagrange 插值配点格式和重心有理插值配点格式的数值解图及误差分布图, 分别如图 1, 2 所示. 图 1, 2 中:  $\varphi^h$  为数值解,  $\delta$  为数值解和真解之间的误差.

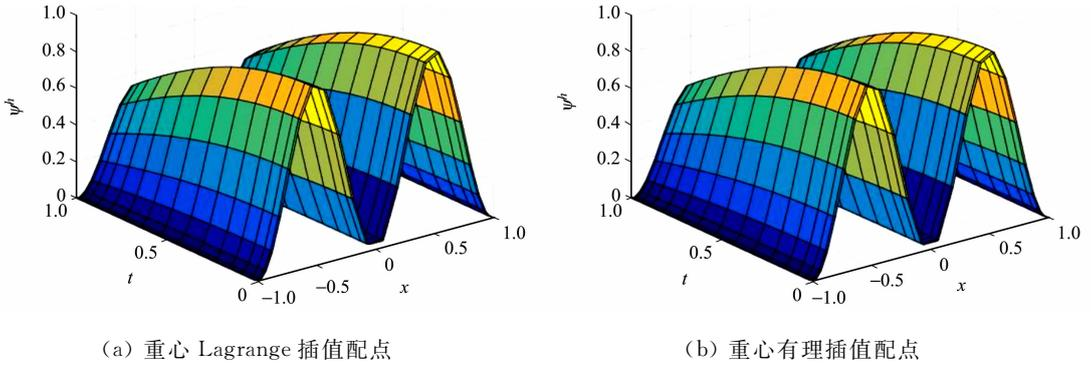


图 1 两种重心插值配点格式的数值解图 ( $M=25, N=15$ )

Fig. 1 Numerical solution graph of two barycentric interpolation collocation formats ( $M=25, N=15$ )

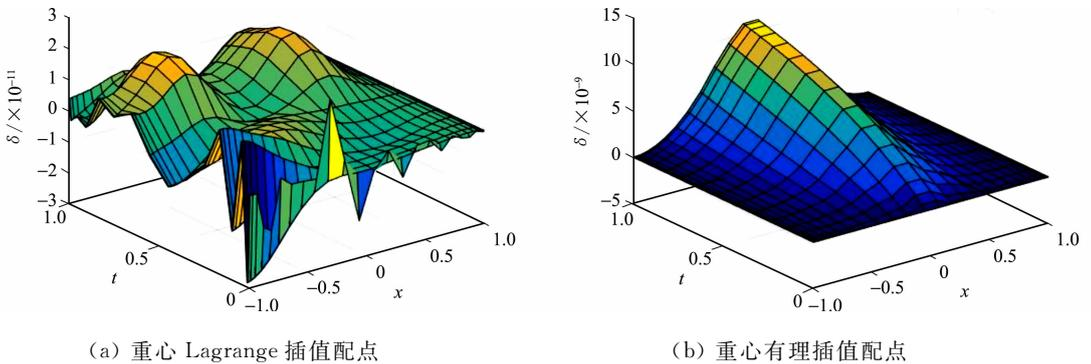


图 2 两种重心插值配点格式的误差分布图 ( $M=25, N=15$ )

Fig. 2 Error distribution diagram of two barycentric interpolation collocation point formats ( $M=25, N=15$ )

由图 1, 2 可知: 两种重心插值配点格式的数值图像几乎一致, 均逼近于真实解, 但重心 Lagrange 插值配点格式的精度更高.

### 2.2 算例 2

为了进一步验证数值格式的有效性, 考虑 Cahn-Hilliard 方程的离散能量函数, 即

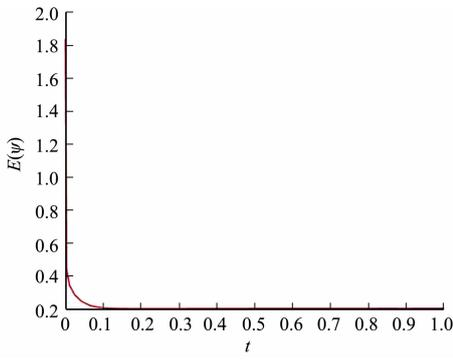
$$E^h(\varphi^n) = \frac{1}{4} \sum_{i=0}^M h_i [(\varphi_i^n)^2 - 1]^2 + \frac{\epsilon^2}{2} \sum_{i=1}^{M-1} h_i \left[ \frac{\varphi_{i+1}^n - \varphi_{i-1}^n}{2h_i} \right]^2. \quad (42)$$

式(42)中:  $\varphi_i^n$  为第  $n$  个时刻, 在  $x$  方向上第  $i$  个节点上的数值解;  $E^h(\varphi^n)$  为第  $n$  个时刻的能量值;  $h_i$  为  $x$  方向上相邻两个 Chebyshev 节点的步长. 取  $x \in [-1, 1], t \in [0, 1]$ , 初值  $\varphi^0 = \sin^2(\pi x)$ , 边界条件为

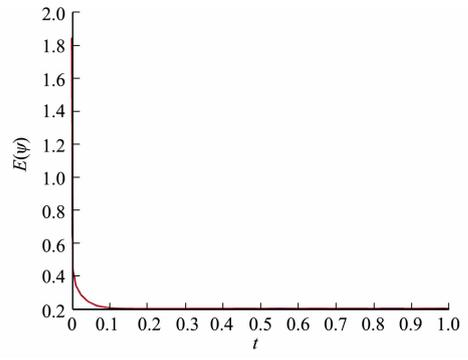
$$\varphi(-1, t) = -1, \quad \varphi(1, t) = 1, \quad \varphi'(-1, t) = \varphi'(1, t) = 0.$$

取  $M=30, N=30$ , 在不同  $\epsilon^2$  取值下, 两种重心插值配点格式求解 Cahn-Hilliard 方程对应的能量递减图及数值解图, 分别如图 3, 4 所示.

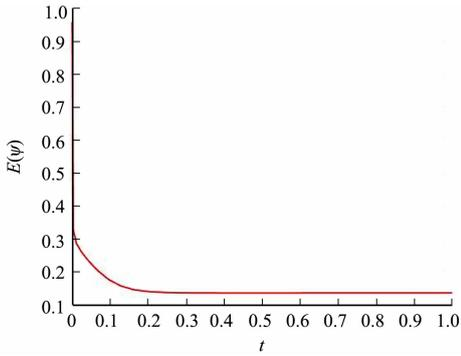
由图 3 可知: 两种重心插值配点格式均满足能量递减规律, 即随着时间  $t$  递增, 能量函数  $E(\varphi)$  不断递减, 最后达到稳定状态; 当  $\epsilon^2$  变小时, 趋于稳定状态的时间会变长, 能量值会变小. 由图 4 可知: 不管  $\epsilon^2$  取何值, 重心 Lagrange 插值配点插值效果都更好, 数值解图像更光滑, 两种重心插值配点格式图像最



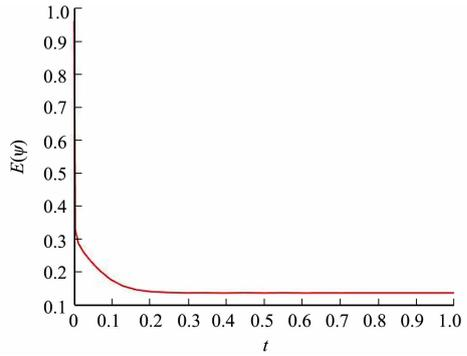
(a) 重心 Lagrange 插值配点( $\epsilon^2=0.09$ )



(b) 重心有理插值配点( $\epsilon^2=0.09$ )



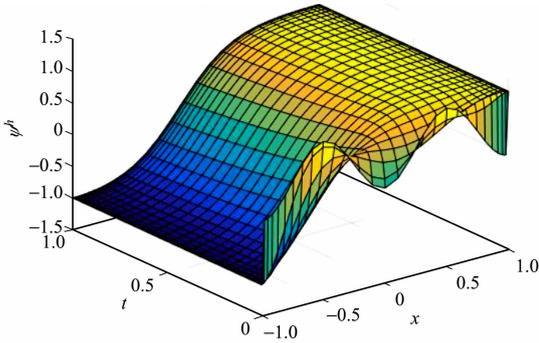
(c) 重心 Lagrange 插值配点( $\epsilon^2=0.04$ )



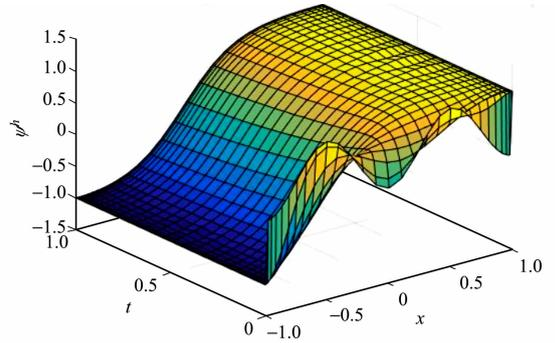
(d) 重心有理插值配点( $\epsilon^2=0.04$ )

图 3 不同  $\epsilon^2$  取值下两种重心插值配点格式的能量递减图( $M=30, N=30$ )

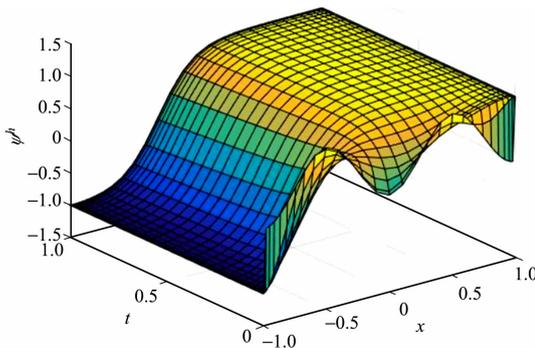
Fig. 3 Energy declining graphs of two barycentric interpolation collocation point formats under different values of  $\epsilon^2$  ( $M=30, N=30$ )



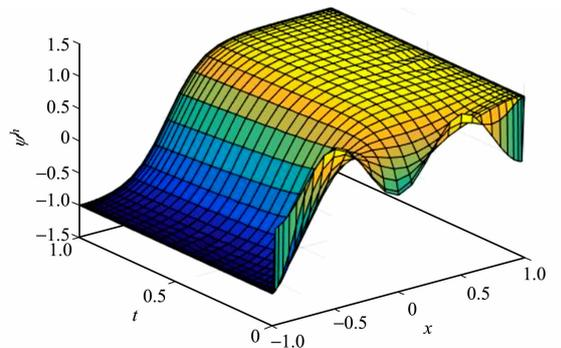
(a) 重心 Lagrange 插值配点( $\epsilon^2=0.09$ )



(b) 重心有理插值配点( $\epsilon^2=0.09$ )



(c) 重心 Lagrange 插值配点( $\epsilon^2=0.04$ )



(d) 重心有理插值配点( $\epsilon^2=0.04$ )

图 4 不同  $\epsilon^2$  取值下两种重心插值配点格式的数值解图( $M=30, N=30$ )

Fig. 4 Numerical solution graph of two barycentric interpolation collocation schemes under different  $\epsilon^2$  values ( $M=30, N=30$ )

终都趋于稳态.

### 3 结束语

利用重心 Lagrange 插值配点格式和重心有理插值配点的一般迭代格式求解 Cahn-Hilliard 方程, 并给出了重心 lagrange 插值的逼近误差. 数值算例比较了两种重心插值配点格式的精度和稳定性. 当剖分节点数较少时, 重心 lagrange 插值精度更高; 当剖分节点数较多时, 重心有理插值配点稳定性更好. 最后, 验证了两种格式均满足能量递减规律. 接下来将进一步研究重心插值配点推广到高阶非线性的问题.

#### 参考文献:

- [1] CAHN J W, HILLIARD J E. Free energy of a nonuniform system I interfacial free energy[J]. *Journal of Chemical Physics*, 1958, 28(2): 258-267. DOI: 10. 1063/1. 1744102.
- [2] ANDERSON D M, MCFADDEN G B, WHEELER A A. Diffuse-interface methods in fluid mechanics[J]. *Annual Review of Fluid Mechanics*, 1998, 30(1): 139-165. DOI: 10. 1146/annurev. fluid. 30. 1. 139.
- [3] YUE Pengtao, FENG J J, LIU Chun, *et al.* A diffuse-interface method for simulating two-phase flows of complex fluids[J]. *Journal of Fluid Mechanics*, 2004, 515: 293-317. DOI: 10. 1017/S0022112004000370.
- [4] SHEN Jie, YANG Xiaofeng, YU Haijun. Efficient energy stable numerical schemes for a phase field moving contact line model[J]. *Journal of Chemical Physics*, 2015, 284(3): 617-630. DOI: 10. 1016/j. jcp. 2014. 12. 046.
- [5] LI Yibao, KIM J. Multiphase image segmentation using a phase-field model[J]. *Computers and Mathematics with Applications*, 2011, 62(2): 737-745. DOI: 10. 1016/j. camwa. 2011. 05. 054.
- [6] LI Yibao, JEONG D, CHOI J, *et al.* Fast local image inpainting based on the Allen-Cahn model[J]. *Digital Signal Processing*, 2015, 37: 65-74. DOI: 10. 1016/j. dsp. 2014. 11. 006.
- [7] DU Qiang, LIU Chun, WANG Xiaoqiang. Simulating the deformation of vesicle membranes under elastic bending energy in three dimensions[J]. *Journal of Computational Physics*, 2006, 212(2): 757-777. DOI: 10. 1016/j. jcp. 2005. 07. 020.
- [8] WU X, VAN ZWIETEN G J, VAN D Z K G. Stabilized second-order convex splitting schemes for Cahn-Hilliard models with application to diffuse-interface tumor-growth models[J]. *International Journal for Numerical Methods in Biomedical Engineering*, 2014, 30(2): 180-203. DOI: 10. 1002/cnm. 2597.
- [9] SUN Zhizhong. A second-order accurate linearized difference scheme for the two-dimensional Cahn-Hilliard equation[J]. *Mathematics of Computation*, 1995, 64(212): 1463-1471. DOI: 10. 1090/S0025-5718-1995-1308465-4.
- [10] WISE S M. Unconditionally stable finite difference, nonlinear multigrid simulation of the Cahn-Hilliard-Hele-Shaw system of equations[J]. *Journal of Scientific Computing*, 2010, 44(1): 38-68. DOI: 10. 1007/s10915-010-9363-4.
- [11] LI Yibao, LEE H G, XIA Binhu, *et al.* A compact fourth-order finite difference scheme for the three-dimensional Cahn-Hilliard equation[J]. *Computer Physics Communications*, 2016, 200: 108-116. DOI: 10. 1016/j. cpc. 2015. 11. 006.
- [12] ELLIOTT C M, RANNER T. Evolving surface finite element method for the Cahn-Hilliard equation[J]. *Numer Math*, 2015, 129(3): 483-534. DOI: 10. 1007/s00211-014-0644-y.
- [13] YAN Yue, CHEN Wenbin, WANG Cheng, *et al.* A second-order energy stable BDF numerical scheme for the Cahn-Hilliard equation[J]. *Communications in Computational Physics*, 2018, 23(2): 572-602. DOI: 10. 4208/cicp. OA-2016-0197.
- [14] CUETO-FELGUEROSO L, PERAIRE J. A time-adaptive finite volume method for the Cahn-Hilliard and Kuramoto-Sivashinsky equations[J]. *Journal of Computational Physics*, 2008, 227(24): 9985-10017. DOI: 10. 1016/j. jcp. 2008. 07. 024.
- [15] CHENG Kelong, WANG Cheng, WISE S M, *et al.* A second-order, weakly energy-stable pseudo-spectral scheme for the Cahn-Hilliard equation and its solution by the homogeneous linear iteration method[J]. *Journal of Scientific Computing*, 2016, 69(3): 1083-1114. DOI: 10. 1007/s10915-016-0228-3.
- [16] HE Liping, LIUYunxian. A class of stable spectral methods for the Cahn-Hilliard equation[J]. *Journal of Computational Physics*, 2009, 228(14): 5101-5110. DOI: 10. 1016/j. jcp. 2009. 04. 011.

- [17] ZHANG Zhengru, QIAO Zhonghua. An adaptive time-stepping strategy for the Cahn-Hilliard equation[J]. *Communications in Computational Physics*, 2012, 11(4): 1261-1278. DOI: 10.4208/cicp.300810.140411s.
- [18] CHENG Yuanzhen, KURGANOV A, QU Zhuolin. Fast and stable explicit operator splitting methods for phase-field models[J]. *Journal of Computational Physics*, 2015, 303: 45-65. DOI: 10.1016/j.jcp.2015.09.005.
- [19] LI Dong, QIAO Zhonghua. On second order semi-implicit Fourier spectral methods for 2D Cahn-Hilliard equations [J]. *Journal of Scientific Computing*, 2017, 70(1): 301-341. DOI: 10.1007/s10915-016-0251-4.
- [20] CHENG Kelong, FENG Wenqiang, WANG Cheng. An energy stable fourth order finite difference scheme for the Cahn-Hilliard equation[J]. *Journal of Computational and Applied Mathematics*, 2019, 362: 574-595. DOI: 10.1016/j.cam.2018.05.039.
- [21] WANG Lin, YU Haijun. An energy stable linear diffusive Crank-Nicolson scheme for the Cahn-Hilliard gradient flow[J]. *Journal of Computational and Applied Mathematics*, 2020, 377: 1-26. DOI: 10.1016/j.amc.2019.06.062.
- [22] ZHANG Jun, JIANG Maosheng. Energy-stable predictor-corrector schemes for the Cahn-Hilliard equation[J]. *Journal of Computational and Applied Mathematics*, 2020, 376: 112832. DOI: 10.1016/j.cam.2020.112832.
- [23] 李淑萍, 王兆清, 唐炳涛. 重心插值配点法求解初值问题[J]. *山东建筑大学学报*, 2007, 22(6): 481-485. DOI: 10.3969/j.issn.1673-7644.2007.06.003.
- [24] BERRUT J P, TREFETHEN L N. Barycentric lagrange interpolation[J]. *SIAM Review*, 2004, 46(3): 501-517. DOI: 10.1137/S0036144502417715.
- [25] FLOATER M S, HORMANN K. Barycentric rational interpolation with no poles and high rates of approximation [J]. *Numerische Mathematik*, 2007, 107(2): 315-331. DOI: 10.1007/s00211-007-0093-y.
- [26] LIU Hongyan, HUANG Jin, PAN Yubin, *et. al.* Barycentric interpolation collocation methods for solving linear and nonlinear high-dimensional Fredholm integral equation[J]. *Journal of Computational and Applied Mathematics*, 2018, 327: 141-154. DOI: 10.1016/j.cam.2017.06.004.
- [27] LUO Weihua, HUANG Tingzhu, GU Xianming, *et. al.* Barycentric rational collocation methods for a class of nonlinear parabolic partial differential equations[J]. *Applied Mathematics Letters*, 2017, 68: 13-19. DOI: 10.1016/j.aml.2016.12.011.
- [28] ORUC O. Two meshless methods based on local radial basis function and barycentric rational interpolation for solving 2D viscoelastic wave equation[J]. *Computers and Mathematics with Applications*, 2020, 79(12): 3272-3288. DOI: 10.1016/j.camwa.2020.01.025.
- [29] 翁智峰, 姚泽丰, 赖淑琴. 重心插值配点法求解 Allen-Cahn 方程[J]. *华侨大学学报(自然科学版)*, 2019, 40(1): 133-140. DOI: 10.11830/ISSN.1000-5013.201806043.
- [30] 邓杨芳, 姚泽丰, 汪精英, 等. 二维 Allen-Cahn 方程的有限差分法/配点法求解[J]. *华侨大学学报(自然科学版)*, 2020, 41(5): 133-140. DOI: 10.11830/ISSN.1000-5013.202001001.
- [31] 赖淑琴, 华之维, 翁智峰. 重心插值配点法求解 Black-Scholes 方程[J]. *聊城大学学报(自然科学版)*, 2020, 33(5): 481-485. DOI: 10.19728/j.issn1672-6634.2020.05.001.
- [32] 李树忱, 王兆清. 高精度无网格重心插值配点法: 算法、程序及工程应用[M]. 北京: 科学出版社, 2012.
- [33] YI Shichao, YAO Linquan. A steady barycentric Lagrange interpolation method for the 2D higher-order time-fractional telegraph equation with nonlocal boundary condition with error analysis[J]. *Numerical Methods for Partial Differential Equations*, 2019, 35(5): 1694-1716. DOI: 10.1002/num.22371.

(责任编辑: 陈志贤 英文审校: 黄心中)